ACS SyntheticBiology

pubs.acs.org/synthbio Letter

A New Biosensor for Stilbenes and a Cannabinoid Enabled by Genome Mining of a Transcriptional Regulator

Huihua Sun, Huimin Zhao,* and Ee Lui Ang*

Cite This: *ACS Synth. Biol.* 2020, 9, 698−705 Read Online

ACCESS | Metrics & More | Article Recommendations | Supporting Information

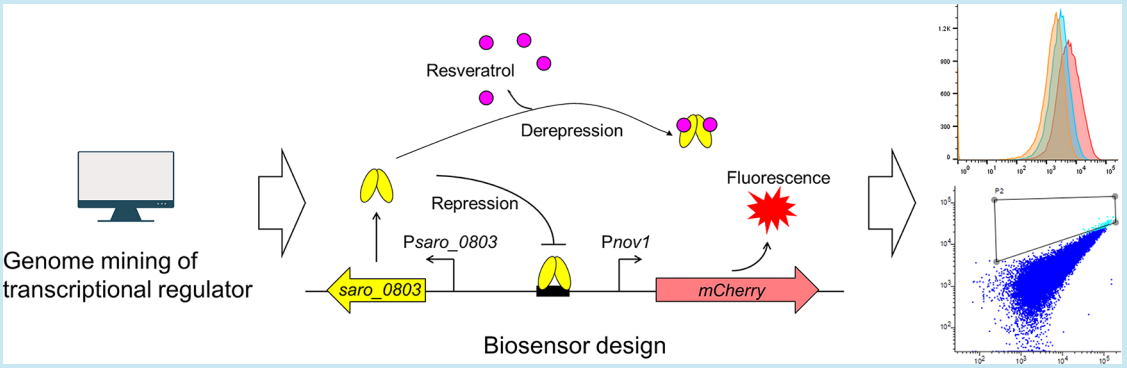

ABSTRACT: *In vivo* biosensors are powerful tools for metabolic engineering and synthetic biology applications. However, the development of biosensors is hindered by the limited number of characterized transcriptional regulators. The versatile sensing abilities of microbes and genome sequences available hold great potential for developing novel biosensors via genome mining for new transcriptional regulators. Here we report the development and engineering of a new stilbene-responsive biosensor discovered by mining the *Novosphingobium aromaticivorans* DSM 12444 genome. The biosensor can distinguish resveratrol from its precursors, *p*-coumaric acid and *trans*-cinnamic acid. Remarkably, it can detect other biologically active stilbenes with resorcinol groups, and cannabidiolic acid with a *β*-resorcylic acid functional group. When coupled to resveratrol biosynthesis enzymes, the biosensor can sense altered resveratrol production in cells, demonstrating a 667-fold enrichment in one round of fluorescence-activated cell sorting. Our biosensor will be potentially applicable to metabolic engineering of microbial cell factories for production of stilbenes and cannabinoids.

KEYWORDS: *biosensor, transcriptional regulator, genome mining, resveratrol, stilbenes, cannabinoid*

Metabolic engineering has enabled microbial cell factories to produce high value chemicals in sustainable and efficient ways.[1−3] Combinatorial optimization strategies such as *in vivo* evolution,[4,5] genome engineering,[6−8] and directed protein evolution[9,10] usually require huge screening capacities. However, lack of high-throughput screening methods targeting the chemicals of interest remains the bottleneck to the successful application of these powerful metabolic engineering tools. To address this problem, it is important to develop diverse biosensors[11−14] to specifically link the metabolite production to an output, which enables high-throughput screening via powerful selection tools such as fluorescence-activated cell sorting (FACS). Microbial transcription factors (TFs) have been widely exploited for whole-cell biosensor designs,[15] but the biosensors reported are typically based on a limited number of previously well-characterized TFs, which hinders rapid access to novel biosensors. Given an almost inexhaustible repertoire of small molecules sensed by bacteria and the huge number of genome sequences available, it is attractive to develop novel biosensors via genome mining of new TF-promoter pairs.

Stilbenes or stilbenoids are a class of naturally occurring phenolic compounds often produced by plants to protect themselves against microbial infection.[16] The most commercially relevant stilbene, resveratrol, has been widely studied due to its versatile biological activities which include cardiovascular protection and anticancer, antioxidant, antiaging, anti-inflammatory, and antidiabetic effects.[17−19] Resveratrol has become an attractive ingredient for the food, nutraceutical, and cosmetic industries.[20] The rhizome or root of Japanese knotweed has been used as a major source for resveratrol ingredients in the growing nutraceutical market. However,

Received: November 1, 2019
Published: February 20, 2020

https://dx.doi.org/10.1021/acssynbio.9b00443
ACS Synth. Biol. 2020, 9, 698−705

knotweed extracts contain as low as 50% of *trans*-resveratrol and also contain emodin with a laxative effect.[20] As the demand for resveratrol is growing rapidly, resveratrol production with lower cost and higher purity is highly desired.

The biosynthetic pathway of *trans*-resveratrol in plants begins with formation of *p*-coumaric acid from tyrosine or phenylalanine, or both. *p*-Coumaric acid is then converted to coumaroyl-coenzyme A (CoA) by 4-coumarate:CoA ligase (4CL). Finally, a type III polyketide synthase (PKS), stilbene synthase (STS), condenses one unit of coumaroyl-CoA and three units of malonyl-CoA into resveratrol (Scheme 1A).

Scheme 1. Schematic Representation of Resveratrol Synthesis and Degradation

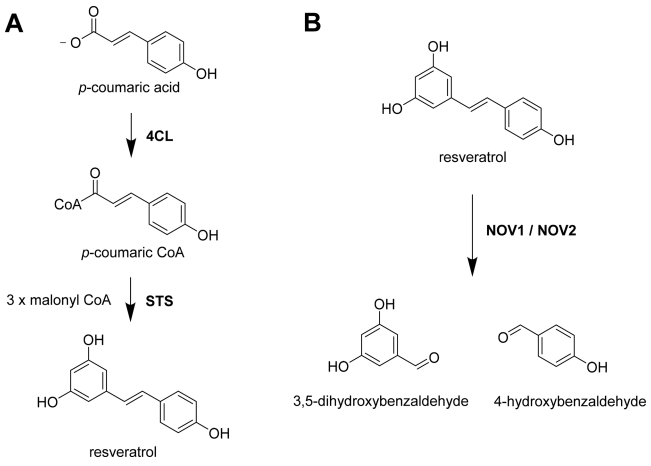

(A) Biosynthesis of resveratrol from *p*-coumaric acid. (B) Enzymatic degradation of resveratrol to 3,5-dihydroxybenzaldehyde and 4-hydroxybenzaldehyde.

Many efforts have been made in the biosynthesis of resveratrol using genetically engineered *Escherichia coli* (*E. coli*)[21] and *Saccharomyces cerevisiae*.[20] Further engineering of microbial strains for resveratrol production would be facilitated by the development of a resveratrol biosensor. Recently, Xiong and co-workers engineered the TtgR protein, which is naturally induced by genistein, for altered effector specificity to resveratrol.[22] However, both negative screening against the precursor *p*-coumaric acid and the positive screening against resveratrol had to be performed repeatedly, which is time-consuming. A naturally occurring transcriptional regulator specifically responsive to resveratrol and other stilbenes has never been reported so far.

In this work, we discovered the first naturally occurring stilbene-responsive TF-promoter pair, introduced the genetic parts into *E. coli*, improved the performance of the resulting biosensor, and characterized the resulting biosensor *in vivo*. Our biosensor with the naturally occurring TF-promoter pair exhibited responses to a broader range of valuable natural products, including stilbenes with a resorcinol group and even a cannabinoid with a β-resorcylic acid functional group. Such a biosensor will potentially enable the development of a high-throughput screening method for metabolic engineering of stilbene-producing or cannabinoid-producing strains in the future.

RESULTS AND DISCUSSION

Genome Mining for a Resveratrol-Responsive TF-Promoter Pair. In bacteria, the expression of the enzymes in the catabolism of some aromatic compounds is often regulated by the transcriptional regulators that respond to the presence of the catabolic substrates or intermediates.[23−25] In light of this, we first searched for reported bacterial enzymes capable of degrading stilbenes. Marasco and Schmidt-Dannert identified two carotenoid cleavage oxygenase homologues, NOV1 and NOV2 in the genome of the noncarotenogenic bacterium *Novosphingobium aromaticivorans* DSM 12444.[26] NOV1 and NOV2 were demonstrated to cleave the interphenyl α-β double bond of resveratrol (Scheme 1B) and three stilbene derivatives (piceatannol, rhapontigenin, and rhaponticin) via a monooxygenase reaction mechanism. *Novosphingobium* is known for its ability to degrade various aromatic compounds.[27,28]

We surveyed the genome sequence of *Novosphingobium aromaticivorans* DSM 12444 and found the gene *saro_0803* encoding a putative transcriptional regulator located directly upstream of *nov1* (Figure 1A). Saro_0803 was predicted to be

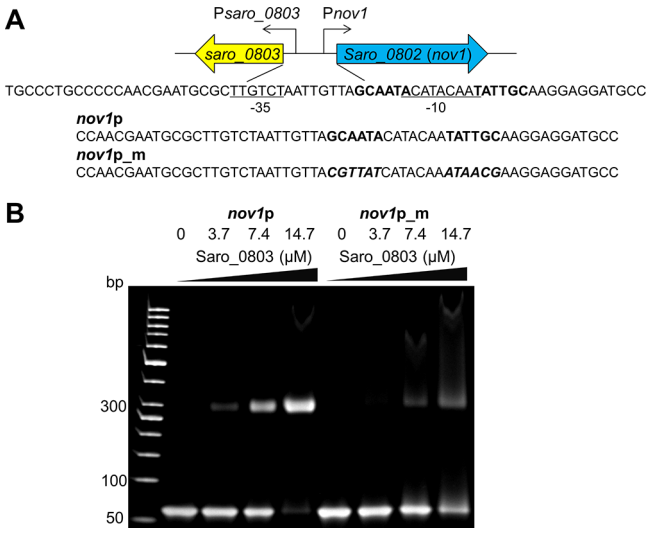

Figure 1. EMSA analysis of the newly discovered TF-promoter pair. (A) The gene *saro_0803*, *saro_0802* (*nov1*) and intergenic sequence found in the genome of *Novosphingobium aromaticivorans* DSM 12444; and DNA sequences used for the EMSA analysis. The inverted repeat is indicated in bold characters. The italicized characters indicate the nucleotide substituted. (B) EMSA analysis of the TF binding site. A varying concentration of Saro_0803 was incubated with 2.5 μM promoter DNA. (C) Release of DNA upon binding of resveratrol to Saro_0803.

a transcriptional regulator belonging to the multiple antibiotics resistance regulator (MarR) family, which includes TFs responsible for the resistance to antibiotics and the catabolism of aromatic compounds.[29] Pairwise sequence alignment shows that SACE_0803 (Accession number: ABD25248) shares 20.6%/37.0% amino acid identity/similarity with *E. coli* MarR (Accession number: WP_089614970). Transcriptions of *saro_0803* and *nov1* are in opposite directions. Sequence analysis of the *nov1* promoter by BPROM[30] indicated that it possesses the canonical −10 and −35 boxes, ACATACAA and TTGTCT. Notably, the *nov1* promoter also contains an inverted repeat separated by a 7-bp spacer, GCAATA-------TATTGC, overlapping the predicted −10 box (Figure 1A).

https://dx.doi.org/10.1021/acssynbio.9b00443
ACS Synth. Biol. 2020, 9, 698−705

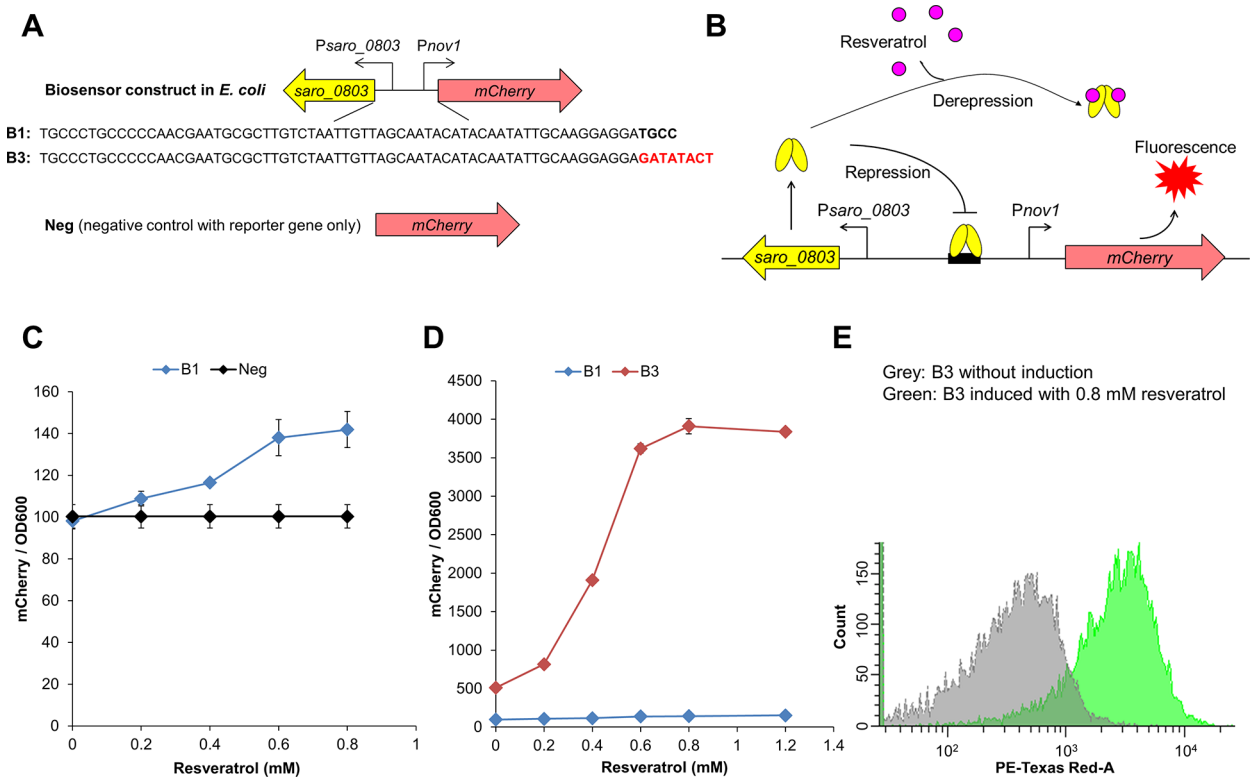

Figure 2. Biosensor constructs with a TF-promoter pair in *E. coli*. (A) The construction of the biosensor (B1 and B3) and the negative control (Neg). (B) Proposed scheme of the biosensor with Saro_0803 regulatory system. (C) Dose responses for B1 and the negative control. (D) Dose responses for B1 and B3. (E) mCherry fluorescence histogram generated by flow cytometry. The *x* axis is in logical scaling. Data in panels C and D represent mean ± s.d. of three biological replicates.

Such inverted repeats are characteristic of the nucleotide sequences recognized by MarR family transcriptional regulators.[25,31,32] To demonstrate that this inverted repeat is the TF binding site, electrophoretic mobility shift assay (EMSA) was performed with purified Saro_0803 and the 58-bp *nov1* promoter DNA (*nov1*p) or *nov1*pm, in which the 12 nucleotides (nt) of the inverted repeat were substituted (Figure 1A). In gel shift assays, increasing amounts of the *nov1*p fragment were shifted in the presence of increasing concentrations of Saro_0803 (0, 3.7, 7.4, and 14.7 μM) (Figure 1B). But the same amount of protein did not obviously bind well with *nov1*pm (Figure 1B). This observation indicates that the inverted repeat is required for Saro_0803 to bind the *nov1* promoter. It also suggests that the binding of Saro_0803 to the inverted repeat that overlaps the −10 promoter sequence may suppress the transcription of the *nov1* gene.

To examine if the binding of resveratrol to the regulator Saro_0803 could release the promoter DNA *in vitro*, 500 μM resveratrol was incubated with the mixture of 5 μM *nov1*p and 14.7 μM Saro_0803. The EMSA analysis showed that a small portion of *nov1*p DNA was released from Saro_0803 in the presence of resveratrol (Figure S2). Taken together, the binding of Saro_0803 to a cognate binding sequence on the *nov1* promoter and the weakened binding in the presence of resveratrol suggest the role of Saro_0803 in stilbene-responsive regulation of the expression of the stilbene-degrading enzyme NOV1. Therefore, we next investigated the possibility of applying this TF-promoter pair as an *in vivo* biosensor for resveratrol detection.

Construction of a Resveratrol Biosensor Using the TF-Promoter Pair in *E. coli*. To construct a resveratrol biosensor in *E. coli*, the gene sequence of *saro_0803* was codon-optimized for expression in *E. coli*, and the intergenic bidirectional promoter sequence was utilized, with the reporter gene *mCherry* substituting the *nov1* gene (Figure 2A,B). The biosensor construct B1 contains the original intergenic promoter sequence, and the negative control (Neg) was constructed with the reporter gene only. The *E. coli* cells with B1 showed response to the addition of resveratrol, while no response was observed for Neg (Figure 2C).

To ensure proper spacing between the ribosomal binding site (RBS) and the initiation codon for optimal mCherry expression in *E. coli*, the 8-nt sequence GATATACC replacing the original TGCC sequence was inserted between the RBS and the start codon for *mCherry*, generating the biosensor B2 with a higher induction fold (Figure S3). In addition, the biosensor B3 containing a random mutation from GATATACC to GATATACT in the intergenic region (Figure 2A) showed an even higher induction fold than B2 (Figure S2). A tight correlation was observed between fluorescence intensity and resveratrol concentration from 0.2 mM to 0.8 mM. Compared to the induction fold of 1.4 for B1, the engineered version B3 showed the induction fold of 7.8 when 0.8 mM resveratrol was added (Figure 2D).

To survey the heterogeneity of the cell population and the potential to use this biosensor to screen at the single cell level, *E. coli* cells carrying B3 plasmid induced with 0.8 mM resveratrol and without induction were analyzed by flow cytometry. The histogram showed low fluorescence for cells without induction, while the addition of 0.8 mM resveratrol significantly shifted the fluorescence of the cell population to higher mCherry fluorescence (Figure 2E). This result indicates

https://dx.doi.org/10.1021/acssynbio.9b00443
ACS Synth. Biol. 2020, 9, 698−705

the potential of applying the whole-cell biosensor for screening at a single cell level.

We then probed if the change of the expression level of Saro_0803 could affect the performance of the biosensor. The modification of start codon[33] and RBS[34] could affect the protein translation efficiency, thus the protein expression level. The quantitative fluorescence measurement showed that the start codon change led to lower protein expression level (Figure S4A). B3 v2 was generated with the change of the start codon for *saro_0803* from ATG to TTG. B3 v3 was generated with both the above start codon change and the RBS change for *saro_0803* from AGGG to AGGT. Unmodified B3 was also named as B3 v1. The dose response curves for these three constructs showed that B3 v2 and B3 v3 were less sensitive to resveratrol than B3 v1 (Figure S4B). It also further proves that Saro_0803 is responsible for the regulation of mCherry expression upon sensing of the resveratrol.

Specificity of the Biosensor. For biosensor-based screening, precursors in the biosynthetic pathway of the desired compound must not activate the biosensor.[11] A specificity test of the biosensor B3 was carried out on the two precursors, *p*-coumaric acid and *trans*-cinnamic acid. At the same time, we also tested other stilbenes (piceatannol, pinosylvin, pterostilbene) and glucosylated derivates (piceid, rhapontin) that were commercially available. 0.8 mM of each compound was added to *E. coli* cells with B3, and the same volume of the solvent DMSO was added as a negative control. Compared to the negative control, the biosensor did not show response to the two precursors, *p*-coumaric acid and *trans*-cinnamic acid (Figure 3). Interestingly, the biosensor also

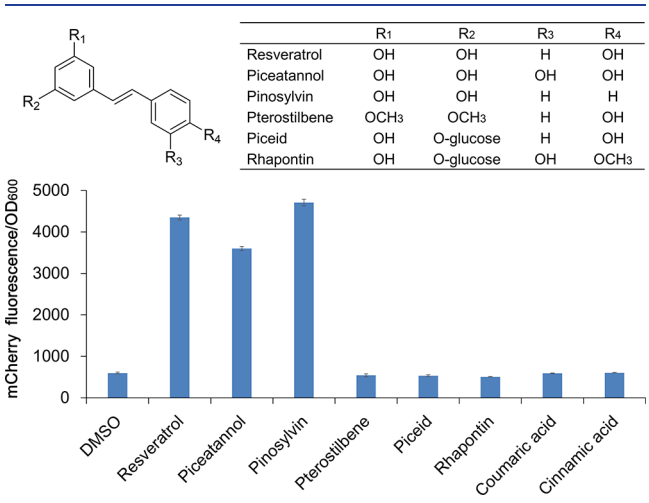

Figure 3. Specificity test of the biosensor B3 on various stilbenes and glucosylated derivatives. The final concentration of each compound was 0.8 mM. DMSO was used as the negative control since all the compounds were dissolved in DMSO. Data represent mean ± s.d. of three biological replicates.

showed comparable response to two other stilbenes, piceatannol and pinosylvin, but not pterostilbene, or the two stilbene glucosides, piceid and rhapontin (Figure 3). Resveratrol, piceatannol, and pinosylvin shared the same resorcinol group (two −OH at R_1 and R_2 positions on one of the aromatic rings as shown in Figure 3). Thus, these data suggest that the *E. coli* cells with B3 are able to detect the stilbenes with a resorcinol group and distinguish the stilbenes from the precursors such as *p*-coumaric acid and *trans*-cinnamic acid. This could potentiate the biosensor for the application in metabolic engineering of cells producing a range of stilbenes with biological activities such as resveratrol,[35−38] piceatannol,[35,37,39] and pinosylvin.[35,37]

To explore the application of the biosensor for other valuable natural products with a resorcinol group, we also tested the biosensor B3 on the three commercially available cannabinoids, (±)-cannabichromene (CBC), cannabidiol (CBD), and cannabidiolic acid (CBDA) (Figure 4A). The biosensor did not show any response to CBC without a resorcinol group. Though both CBD and CBDA are with a resorcinol group, the biosensor only showed response to CBDA with an additional carboxyl group (Figure 4B). The histogram generated by flow cytometry showed that the addition of 40 mg/L CBDA significantly shifted the fluorescence of the cell population to higher mCherry fluorescence (Figure 4C). This result indicates the potential of the biosensor to detect other valuable natural products with resorcinol groups, not limited to stilbenes. The biosensor could be applied for screening of CBDA-producing strains at a single cell level and may also be used to discover new natural products with a resorcinol group.

Response of the Biosensor to Altered Resveratrol Production. To validate if the biosensor is able to sense the resveratrol produced within the cells, two enzymes from the resveratrol biosynthetic pathways, stilbene synthase (STS) and *p*-coumarate:CoA ligase (4CL) were heterologously expressed under GAP promoter (promoter of the *gapA* gene encoding glyceraldehyde-3-phosphate dehydrogenase in *E. coli*). Both STS from *Vitis vinifera* (Genbank accession No. EF192465.1) and 4CL from *Arabidopsis thaliana* (Genbank accession No. U18675.1) were codon optimized for *E. coli* expression and cloned to the same plasmid for the biosensor B3 (Figure S5). Two constructs, B3-STS4CL v1 and B3-STS4CL v2 were generated with the only difference at the intergenic sequence between STS and 4CL (Figure 5A). After culturing in the presence of 1 g/L *p*-coumaric acid at 30 °C for 1 day, B3-STS4CL v1 produced 7.07 μM resveratrol, while B3-STS4CL v2 produced 192.27 μM resveratrol. No resveratrol production was detected for the strain B3 without expression of STS and 4CL. Impressively, the high-resveratrol-producing strain B3-STS4CL v2 showed a higher fluorescence signal than the low-resveratrol-producing strain B3-STS4CL v1 (Figure 5B). The strain B3 without resveratrol production showed even lower fluorescence signal than B3-STS4CL v1, which also indicates the sensitivity of the biosensor that can differentiate between the strains with 0 and 7.07 μM resveratrol production. These results demonstrate that the biosensor can respond to altered resveratrol production within the cell.

Next, we wanted to demonstrate that the biosensor can be applied for high throughput screening. After culturing in the presence of 1 g/L *p*-coumaric acid for 1 day, the strain B3-STS4CL v1 and B3-STS4CL v2 were mixed at the ratio of 1000 to 1 for sorting by FACS. The gate was set for singlet populations to sort top 0.2% high fluorescent cells with various cell sizes (Figure 5C). A total of 8000 cells were collected into the YM9-CM medium and cultured for 2 days. After culturing, the sorted cells exhibited higher mCherry fluorescence than the cells before sorting (Figure 5D). In the end, 66.67% cells were identified as the strain B3-STS4CL v2 from 48 colonies (Figure S6), suggesting a 667-fold enrichment by only one round of sorting. This FACS demonstration offers the potential of using the biosensor for screening of high-resveratrol-

https://dx.doi.org/10.1021/acssynbio.9b00443
ACS Synth. Biol. 2020, 9, 698−705

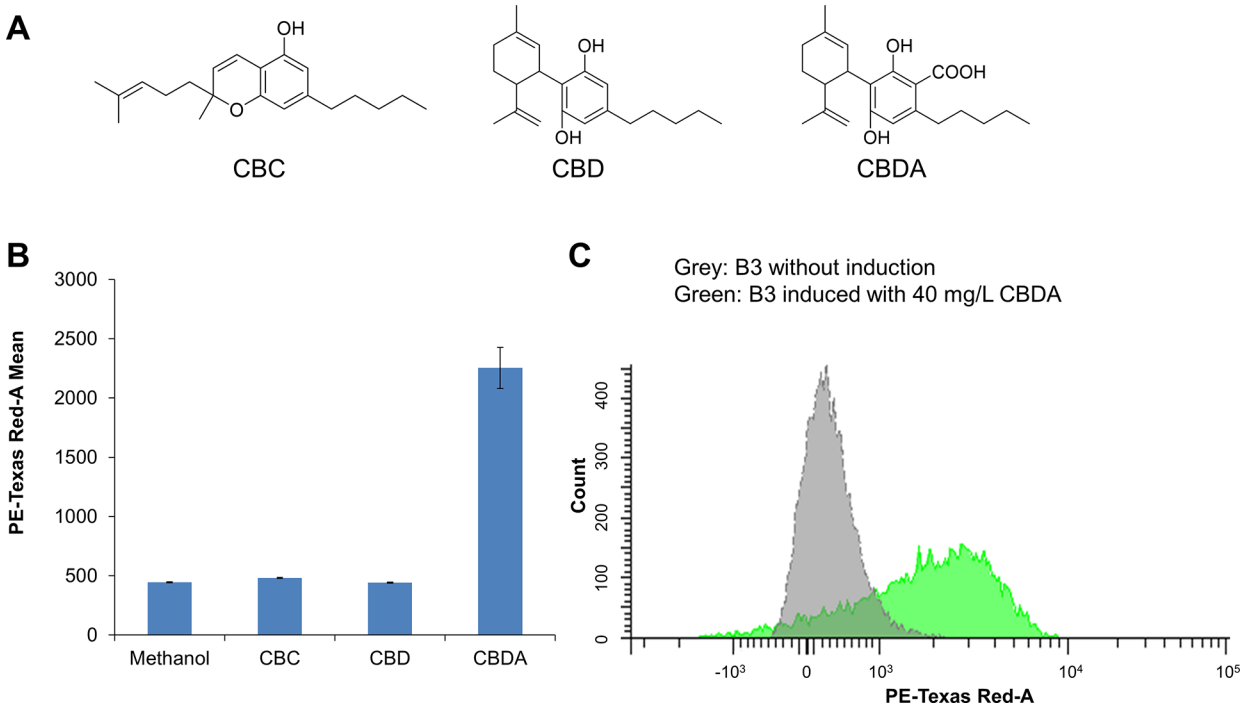

Figure 4. Additional specificity test of the biosensor B3 on three commercially available cannabinoids. (A) Structure scheme of the three cannabinoids. (B) Test of B3 to 40 mg/L CBC, CBD and CBDA. Methanol was used as the negative control since all the compounds were dissolved in methanol. (C) mCherry fluorescence histogram generated by flow cytometry. The *x*-axis is in biexponential scaling.

producing strains via enzyme, pathway, or genome engineering in the future.

This work demonstrated a strategy for the development of whole-cell biosensor, which starts from the genome mining for potential transcriptional regulator responsive to the target compound. It overcomes the dependence on the availability of previously characterized TFs and expedites the finding of novel biosensors, which is a critical tool for the development of high-throughput screening for engineering of cell factories producing target compounds. The biosensor with naturally occurring TF can distinguish resveratrol from the precursors, *p*-coumaric acid and *trans*-cinnamic acid. Other biologically active stilbenes that share a resorcinol group with resveratrol, such as piceatannol and pinosylvin can also be detected. Furthermore, a cannabinoid with β-resorcylic acid functional group can also be recognized by the biosensor. Recently, Luo and co-workers reported the complete biosynthesis of natural and unnatural cannabinoids in yeast.[40] Thus, the biosensor we report expands the detection repertoire for biologically important high-value natural products. And it is intriguing to decipher how the newly discovered Saro_0803 is able to sense these compounds. The biosensor might also be useful in the discovery of novel natural products with resorcinol or β-resorcylic acid functional group.

We also demonstrate that our biosensor responds to altered resveratrol production and one round of FACS gives 667-fold enrichment. This suggests the possible application of the biosensor in high throughput screening during directed evolution of enzymes, pathways, and genomes. One of the key characteristics that needs to be improved is the dynamic range of the biosensor responsive to resveratrol, which will make the cell sorting more efficient. It could be achieved by promoter optimization or even engineering of the regulator in the future. Iterative rounds of sorting may also help achieve higher enrichment for the real library screening in the future. Additionally, one of the big challenges is the transfer of the TF-based biosensor from bacteria to yeast cell factories, although successful adaptation of bacterial transcriptional regulator to yeast has been reported.[41−43] Thus, our whole-cell biosensor using the newly discovered TF-promoter pair for the detection of stilbenes and a cannabinoid will expedite and facilitate the development of efficient strains for production of a broader range of valuable natural products.

METHODS

Culturing and Testing of Whole-Cell Biosensors. *E. coli* strains were inoculated and grown overnight in 2 mL of Luria−Bertani (LB) medium with 50 μg/mL kanamycin at 37 °C, 250 rpm. The next day, 20 μL of the overnight cell culture was inoculated into 2 mL of LB medium with 50 μg/mL kanamycin. For dose response and specificity tests, each diluted culture was first incubated at 37 °C, 250 rpm for 3 h. Then the inducer was added to the cell culture. The culture was further incubated at 37 °C, 250 rpm for 2 h. For mCherry expression tests, each diluted culture was incubated at 37 °C, 250 rpm for 5 h.

A sampling of 100 μL of each cell culture was transferred to a 96-well, flat-bottom, and clear microplate (Greiner Bio-one, Kremsmünster, Austria). The fluorescence and OD_{600} were determined in a Tecan Infinite M200 Pro mciroplate reader. mCherry fluorescence was measured with excitation at 580 and 620 nm with a gain set to 100. The fluorescence intensity was normalized to cell density that was determined by measuring the absorbance at 600 nm using the same microplate reader.

Flow Cytometry. A volume of 200 μL of each cell culture was transferred into a 5 mL polystyrene round-bottom FALCON tube. Following, 400 μL of phosphate-buffered saline buffer was added and mixed to dilute the sample by

https://dx.doi.org/10.1021/acssynbio.9b00443
ACS Synth. Biol. 2020, 9, 698−705

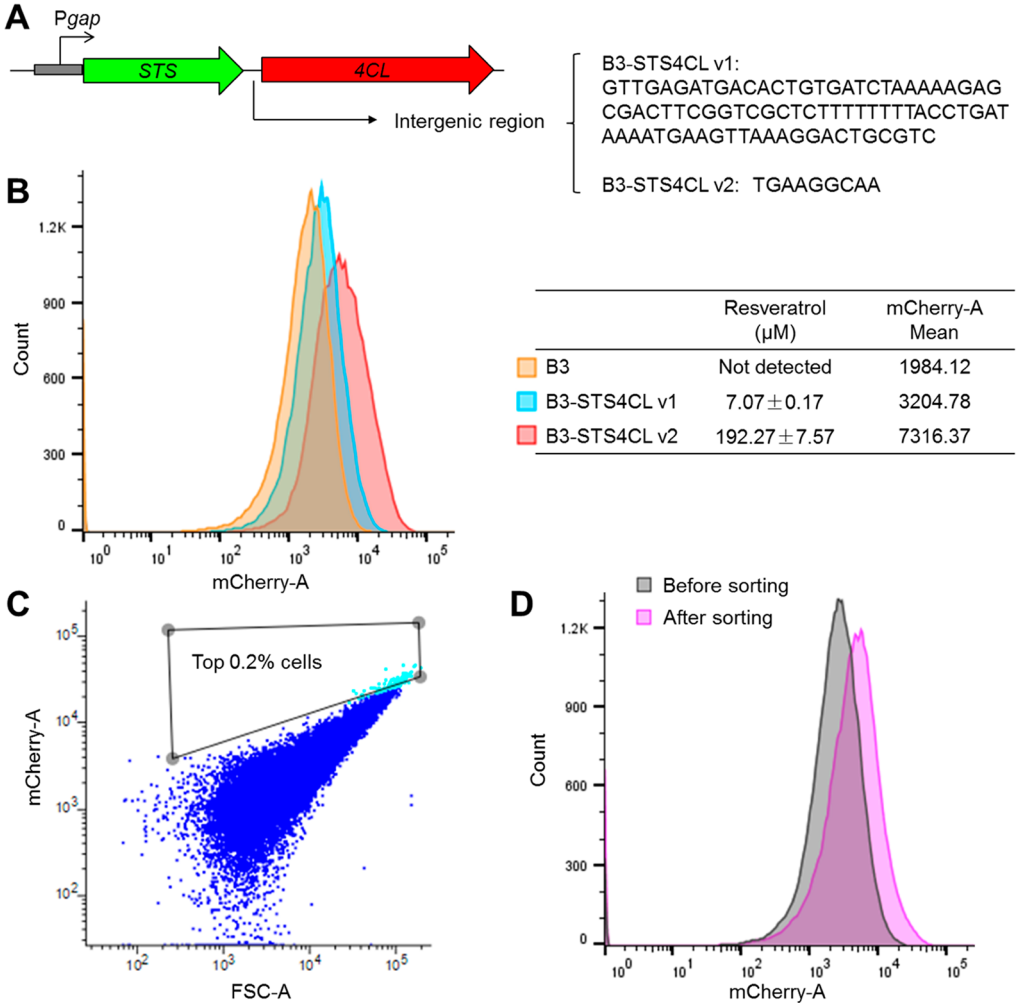

	Resveratrol (μM)	mCherry-A Mean
B3	Not detected	1984.12
B3-STS4CL v1	7.07±0.17	3204.78
B3-STS4CL v2	192.27±7.57	7316.37

Figure 5. Biosensor validation in strains with varied resveratrol production abilities by FACS. (A) The stilbene synthase (STS) and 4-coumarate:CoA ligase (4CL) were expressed under the constitutive GAP promoter. Two different constructs were generated with different intergenic sequence between STS and 4CL, leading to varied resveratrol production after culturing in the presence of 1 g/L *p*-coumaric acid at 30 °C for 1 day. (B) FACS analysis of *E. coli* strain B3, B3-STS4CL v1, and B3-STS4CL v2. The mCherry fluorescence histagrams and mCherry-A mean values were based on the recording of 50 000 events by FACS. The resveratrol produced by the corresponding cell cultures were based on three runs by HPLC. (C) Gating of the singlets population to sort the top 0.2% cells from the mixed cells with the ratio of strain B3-STS4CL v1 to strain B3-STS4CL v2 at 1000 to 1. (D) The sorted cells were amplified and compared with the initial mixed cells by FACS. The *x*-axis is in logarithmic scaling.

three times. Flow cytometric measurements were performed on a 5-laser Becton Dickinson (BD) (Franklin Lakes, New Jersey, United States) LSRII flow cytometer with 561 nm excitation from a yellow-green solid-state laser. mCherry fluorescence was detected using a 561 nm long-pass and a 610/20 nm band-pass filter set (PETxRd). Forward-scatter (FSC)-area (*A*) versus side-scatter (SSC)-A was observed, and the gate was set to exclude dead cells. SSC-height (*H*) vs SSC-weight (*W*) and FSC-H vs FSC-W were observed, and the gate was set to exclude doublets. Data were analyzed using BD DIVA 7.0 software.

Cell Sorting. Cell sorting was performed using the BD FACSMelody cell sorter with a 100 μM nozzle. Fluorescence was excited at 488 nm, and the fluorescence emission was detected using a 586/42 nm band-pass filter. *E. coli* cells were first inoculated and grown overnight in 2 mL of LB medium with 50 μg/mL kanamycin at 37 °C, 250 rpm. The next day, 20 μL of the overnight cell culture was inoculated into 2 mL of YM9-CM medium (1X M9 salts, 10 g/L yeast extract, 3% glycerol, 42 g/L MOPS, 1 g/L *p*-coumaric acid, 1 g/L malonic acid, pH 7.0) with 50 μg mL/kanamycin. The diluted culture was incubated at 37 °C, 250 rpm for 1 day. Then strain B3-STS4CL v1 and strain B3-STS4CL v2 were mixed at a ratio of 1000 to 1, as measured by OD_{600}. A volume of 300 μL of culture was diluted with 900 μL of sterile phosphate-buffered saline (PBS), and this mixture was filtered through a 35 μm nylon mesh into a polystyrene tube, which was used immediately for FACS. A 488 nm blue solid state laser was used to detect mCherry fluorescence with a 560 nm long-pass and a 586/42 nm band-pass filter set. As mentioned above, gates were set to exclude dead cells and doublets. The final gate was set based on the observation of FSC-A (a parameter for cell size) against mCherry-A so that high-fluorescence cells with various sizes can be selected. An amount of 5000 cells was collected into 2 mL of YM9-CM medium and amplified through overnight culturing at 37 °C, 250 rpm.

An additional description of methods (chemicals, plasmid construction, expression, and purification of Saro_0803, EMSA, HPLC analysis) can be found in the Supporting Information.

https://dx.doi.org/10.1021/acssynbio.9b00443
ACS Synth. Biol. 2020, 9, 698−705

■ ASSOCIATED CONTENT

Supporting Information

The Supporting Information is available free of charge at https://pubs.acs.org/doi/10.1021/acssynbio.9b00443.

Methods; Figure S1−S6, Table S1; DNA sequences of plasmids (PDF)

■ AUTHOR INFORMATION

Corresponding Authors

Huimin Zhao − *Institute of Chemical and Engineering Sciences (ICES), Agency for Science, Technology and Research (A*STAR), 138669, Singapore; Department of Chemical and Biomolecular Engineering, University of Illinois at Urbana−Champaign (UIUC), Urbana, Illinois 61801, United States;* orcid.org/0000-0002-9069-6739; Email: zhao5@illinois.edu

Ee Lui Ang − *Institute of Chemical and Engineering Sciences (ICES), Agency for Science, Technology and Research (A*STAR), 138669, Singapore;* orcid.org/0000-0002-3070-8056; Email: ang_ee_lui@ices.a-star.edu.sg

Author

Huihua Sun − *Institute of Chemical and Engineering Sciences (ICES), Agency for Science, Technology and Research (A*STAR), 138669, Singapore*

Complete contact information is available at: https://pubs.acs.org/10.1021/acssynbio.9b00443

Notes

The authors declare no competing financial interest.

■ ACKNOWLEDGMENTS

We thank the Agency for Science, Technology and Research, Singapore for supporting various research projects in the Metabolic Engineering Research Laboratory (MERL) through the Visiting Investigator Programme to Professor Huimin Zhao [1535j00137 to H.Z]. This work was supported by the National Research Foundation Singapore [NRF2013-THE001-095]. We also thank the members of MERL, especially Dr Yifeng Wei, for their comments.

■ REFERENCES

(1) Nielsen, J., and Keasling, J. D. (2016) Engineering cellular metabolism. *Cell 164* (6), 1185−1197.

(2) Du, J., Shao, Z., and Zhao, H. (2011) Engineering microbial factories for synthesis of value-added products. *J. Ind. Microbiol. Biotechnol. 38* (8), 873−90.

(3) Liao, J. C., Mi, L., Pontrelli, S., and Luo, S. (2016) Fuelling the future: microbial engineering for the production of sustainable biofuels. *Nat. Rev. Microbiol. 14* (5), 288−304.

(4) Chou, H. H., and Keasling, J. D. (2013) Programming adaptive control to evolve increased metabolite production. *Nat. Commun. 4*, 2595.

(5) Crook, N., Abatemarco, J., Sun, J., Wagner, J. M., Schmitz, A., and Alper, H. S. (2016) In vivo continuous evolution of genes and pathways in yeast. *Nat. Commun. 7*, 13051.

(6) Bao, Z., HamediRad, M., Xue, P., Xiao, H., Tasan, I., Chao, R., Liang, J., and Zhao, H. (2018) Genome-scale engineering of *Saccharomyces cerevisiae* with single-nucleotide precision. *Nat. Biotechnol. 36* (6), 505−508.

(7) Jakociunas, T., Bonde, I., Herrgard, M., Harrison, S. J., Kristensen, M., Pedersen, L. E., Jensen, M. K., and Keasling, J. D. (2015) Multiplex metabolic pathway engineering using CRISPR/Cas9 in *Saccharomyces cerevisiae*. *Metab. Eng. 28*, 213−222.

(8) Lian, J., HamediRad, M., Hu, S., and Zhao, H. (2017) Combinatorial metabolic engineering using an orthogonal tri-functional CRISPR system. *Nat. Commun. 8* (1), 1688.

(9) Molina-Espeja, P., Vina-Gonzalez, J., Gomez-Fernandez, B. J., Martin-Diaz, J., Garcia-Ruiz, E., and Alcalde, M. (2016) Beyond the outer limits of nature by directed evolution. *Biotechnol. Adv. 34* (5), 754−67.

(10) Porter, J. L., Rusli, R. A., and Ollis, D. L. (2016) Directed evolution of enzymes for industrial biocatalysis. *ChemBioChem 17* (3), 197−203.

(11) Rogers, J. K., Taylor, N. D., and Church, G. M. (2016) Biosensor-based engineering of biosynthetic pathways. *Curr. Opin. Biotechnol. 42*, 84−91.

(12) Zhang, J., Jensen, M. K., and Keasling, J. D. (2015) Development of biosensors and their application in metabolic engineering. *Curr. Opin. Chem. Biol. 28*, 1−8.

(13) Eggeling, L., Bott, M., and Marienhagen, J. (2015) Novel screening methods−biosensors. *Curr. Opin. Biotechnol. 35*, 30−6.

(14) Lin, J. L., Wagner, J. M., and Alper, H. S. (2017) Enabling tools for high-throughput detection of metabolites: metabolic engineering and directed evolution applications. *Biotechnol. Adv. 35* (8), 950−970.

(15) Cheng, F., Tang, X. L., and Kardashliev, T. (2018) Transcription Factor-Based Biosensors in High-Throughput Screening: Advances and Applications. *Biotechnol. J. 13* (7), No. e1700648.

(16) Riviere, C., Pawlus, A. D., and Merillon, J. M. (2012) Natural stilbenoids: distribution in the plant kingdom and chemotaxonomic interest in Vitaceae. *Nat. Prod. Rep. 29* (11), 1317−33.

(17) Elshaer, M., Chen, Y., Wang, X. J., and Tang, X. (2018) Resveratrol: An overview of its anti-cancer mechanisms. *Life Sci. 207*, 340−349.

(18) Li, J., Zhang, C. X., Liu, Y. M., Chen, K. L., and Chen, G. (2017) A comparative study of anti-aging properties and mechanism: resveratrol and caloric restriction. *Oncotarget 8* (39), 65717−65729.

(19) de Sa Coutinho, D., Pacheco, M. T., Frozza, R. L., and Bernardi, A. (2018) Anti-inflammatory effects of resveratrol: mechanistic insights. *Int. J. Mol. Sci. 19* (6), 1812.

(20) Li, M., Kildegaard, K. R., Chen, Y., Rodriguez, A., Borodina, I., and Nielsen, J. (2015) De novo production of resveratrol from glucose or ethanol by engineered *Saccharomyces cerevisiae*. *Metab. Eng. 32*, 1−11.

(21) Lim, C. G., Fowler, Z. L., Hueller, T., Schaffer, S., and Koffas, M. A. (2011) High-yield resveratrol production in engineered *Escherichia coli*. *Appl. Environ. Microbiol. 77* (10), 3451−60.

(22) Xiong, D., Lu, S., Wu, J., Liang, C., Wang, W., Wang, W., Jin, J. M., and Tang, S. Y. (2017) Improving key enzyme activity in phenylpropanoid pathway with a designed biosensor. *Metab. Eng. 40*, 115−123.

(23) Fernandez-Lopez, R., Ruiz, R., de la Cruz, F., and Moncalian, G. (2015) Transcription factor-based biosensors enlightened by the analyte. *Front. Microbiol. 6*, 648.

(24) Marin, A. M., Souza, E. M., Pedrosa, F. O., Souza, L. M., Sassaki, G. L., Baura, V. A., Yates, M. G., Wassem, R., and Monteiro, R. A. (2013) Naringenin degradation by the endophytic diazotroph *Herbaspirillum seropedicae* SmR1. *Microbiology 159*, 167−75.

(25) Otani, H., Stogios, P. J., Xu, X., Nocek, B., Li, S.-N., Savchenko, A., and Eltis, L. D. (2016) The activity of CouR, a MarR family transcriptional regulator, is modulated through a novel molecular mechanism. *Nucleic Acids Res. 44* (2), 595−607.

(26) Marasco, E. K., and Schmidt-Dannert, C. (2008) Identification of bacterial carotenoid cleavage dioxygenase homologues that cleave the interphenyl alpha,beta double bond of stilbene derivatives via a monooxygenase reaction. *ChemBioChem 9* (9), 1450−61.

(27) Demanèche, S., Meyer, C., Micoud, J., Louwagie, M., Willison, J. C., and Jouanneau, Y. (2004) Identification and functional analysis of two aromatic-ring-hydroxylating dioxygenases from a *Sphingomonas* strain that degrades various polycyclic aromatic hydrocarbons. *Appl. Environ. Microbiol. 70* (11), 6714−6725.

(28) Shi, T., Fredrickson, J. K., and Balkwill, D. L. (2001) Biodegradation of polycyclic aromatic hydrocarbons by *Sphingomonas*

strains isolated from the terrestrial subsurface. *J. Ind. Microbiol. Biotechnol. 26* (5), 283−9.
(29) Wilkinson, S. P., and Grove, A. (2006) Ligand-responsive transcriptional regulation by members of the MarR family of winged helix proteins. *Curr. Issues. Mol. Biol. 8* (1), 51−62.
(30) V. Solovyev, A. S. (2011) *Automatic annotation of microbial genomes and metagenomic sequences* (Li, R.W. Ed.) Nova Science Publishers.
(31) Deochand, D. K., and Grove, A. (2017) MarR family transcription factors: dynamic variations on a common scaffold. *Crit. Rev. Biochem. Mol. Biol. 52* (6), 595−613.
(32) Grove, A. (2013) MarR family transcription factors. *Curr. Biol. 23* (4), R142−3.
(33) O'Donnell, S. M., and Janssen, G. R. (2001) The initiation codon affects ribosome binding and translational efficiency in *Escherichia coli* of cI mRNA with or without the 5′ untranslated leader. *J. Bacteriol. 183* (4), 1277−1283.
(34) Bonde, M. T., Pedersen, M., Klausen, M. S., Jensen, S. I., Wulff, T., Harrison, S., Nielsen, A. T., Herrgard, M. J., and Sommer, M. O. (2016) Predictable tuning of protein expression in bacteria. *Nat. Methods 13* (3), 233−6.
(35) Akinwumi, B. C., Bordun, K. M., and Anderson, H. D. (2018) Biological activities of stilbenoids. *Int. J. Mol. Sci. 19* (3), 792.
(36) Dvorakova, M., and Landa, P. (2017) Anti-inflammatory activity of natural stilbenoids: A review. *Pharmacol. Res. 124*, 126−145.
(37) Roupe, K. A., Remsberg, C. M., Yanez, J. A., and Davies, N. M. (2006) Pharmacometrics of stilbenes: seguing towards the clinic. *Curr. Clin. Pharmacol. 1* (1), 81−101.
(38) Tsai, H. Y., Ho, C. T., and Chen, Y. K. (2017) Biological actions and molecular effects of resveratrol, pterostilbene, and 3′-hydroxypterostilbene. *J. Food Drug Anal. 25* (1), 134−147.
(39) Piotrowska, H., Kucinska, M., and Murias, M. (2012) Biological activity of piceatannol: leaving the shadow of resveratrol. *Mutat. Res., Rev. Mutat. Res. 750* (1), 60−82.
(40) Luo, X., Reiter, M. A., d'Espaux, L., Wong, J., Denby, C. M., Lechner, A., Zhang, Y., Grzybowski, A. T., Harth, S., Lin, W., Lee, H., Yu, C., Shin, J., Deng, K., Benites, V. T., Wang, G., Baidoo, E. E. K., Chen, Y., Dev, I., Petzold, C. J., and Keasling, J. D. (2019) Complete biosynthesis of cannabinoids and their unnatural analogues in yeast. *Nature 567* (7746), 123−126.
(41) Umeyama, T., Okada, S., and Ito, T. (2013) Synthetic Gene Circuit-Mediated Monitoring of Endogenous Metabolites: Identification of GAL11 as a Novel Multicopy Enhancer of S-Adenosylmethionine Level in Yeast. *ACS Synth. Biol. 2* (8), 425−430.
(42) Li, S., Si, T., Wang, M., and Zhao, H. (2015) Development of a Synthetic Malonyl-CoA Sensor in Saccharomyces cerevisiae for Intracellular Metabolite Monitoring and Genetic Screening. *ACS Synth. Biol. 4* (12), 1308−15.
(43) Wang, M., Li, S., and Zhao, H. (2016) Design and engineering of intracellular-metabolite-sensing/regulation gene circuits in Saccharomyces cerevisiae. *Biotechnol. Bioeng. 113* (1), 206−15.

https://dx.doi.org/10.1021/acssynbio.9b00443
ACS Synth. Biol. 2020, 9, 698−705